Available online at www.sciencedirect.com
SCIENCE DIRECT®

Journal of the European Ceramic Society 23 (2003) 55–60

www.elsevier.com/locate/jeurceramsoc

Effect of lattice impurities on the thermal conductivity of β-Si_3N_4

Hiroshi Yokota*, Masahiro Ibukiyama

Research Center, Denki Kagaku Kogyo K.K 3-5-1 Asahi-cho, Machida-city, 194-8560 Tokyo, Japan

Received 1 October 2001; received in revised form 4 March 2002; accepted 11 March 2002

Abstract

Effect of impurities in the crystal lattice and microstructure on the thermal conductivity of sintered Si_3N_4 was investigated by the use of high-purity β-Si_3N_4 powder. The sintered materials were fabricated by gas pressure sintering at 1900 °C for 8 and 48 h with addition of 8 wt.% Y_2O_3 and 1 wt.% HFO_2. A chemical analysis was performed on the loose Si_3N_4 grains taken from sintered materials after the chemical treatment. Aluminum was not removed from Si_3N_4 grains, which originated from the raw powder of Si_3N_4. The coarse grains had fewer impurities than the fine grains. Oxygen was the major impurity in the grains, and gradually decreased during grain growth. The thermal conductivity increased from 88 Wm^{-1} K^{-1} (8 h) to 120 Wm^{-1} K^{-1} (48 h) as the impurities in the crystal lattice decreased. Purification by grain growth thus improved the thermal conductivity, but changing grain boundary phases might also influence the thermal conductivity.

Keywords: Grain growth; Grain size; Impurities; Si_3N_4; Thermal conductivity

1. Introduction

In recent years, Haggerty and Lightfoot[1] predicted that pure Si_3N_4 has a high intrinsic thermal conductivity of up to 200 Wm^{-1} K^{-1} at room temperature. Very recently, Watari et al.[2] showed that the thermal conductivity of sintered β-Si_3N_4 single grain is 180 Wm^{-1} K^{-1} parallel to the *c*-axis direction.

This estimation and the realization of such high thermal conductivity for sintered materials, combined with the excellent mechanical properties of Si_3N_4, make it a serious candidate for high-performance IC substrates. Silicon nitride, as presently produced, exhibits a relatively poor thermal conductivity, ranging from 20 to 70 Wm^{-1} K^{-1}, which has been reported for β-Si_3N_4 ceramics fabricated by reaction bonding,[3] chemical vapor deposition,[4] hot pressing[3,5,6] and the hot isostatic pressing method.[7,8]

Recently, a significant increase in the thermal conductivity of sintered β-Si_3N_4 has been achieved by using high-purity raw powders with effective sintering additives. Hirosaki et al.[9,10] achieved high thermal conductivity, up to 120 Wm^{-1} K^{-1}, by annealing sintered materials at 2000–2200 °C for 4 h under high nitrogen pressure (10–100 MPa). Hirao et al.[11] fabricated Si_3N_4 with a highly anisotropic microstructure and exhibiting high thermal conductivity up to 60 Wm^{-1} K^{-1} perpendicular to the hot-pressing direction and 120 Wm^{-1} K^{-1} parallel to the hot pressing direction, by using a rodlike Si_3N_4 seed, followed by tape stacking, hot pressing and subsequent annealing at 1850 °C for 66 h under a nitrogen pressure of 0.9 MPa. Watari et al.[12] further annealed this material at 2500 °C under a nitrogen pressure of 200 MPa, and the thermal conductivity reached 155 and 62 Wm^{-1} K^{-1} in the orientations parallel and perpendicular, respectively, to the tape casting direction. Akimune et al.[13] demonstrated that the apparent thermal conductivity of β-Si_3N_4-grain size relationship in their obtained materials followed the Goldsmid and Penn equation, which predicts thermal conductivity to be proportional to the 1/2 power of grain size.

These results suggest that the thermal conductivity of sintered Si_3N_4 is closely related to the microstructure due to grain growth. However, Watari et al.[14] reported that the thermal conductivity of Si_3N_4 at room temperature is independent of grain size, but controlled by the internal defect structure of the grains such as point defects and dislocations. Kitayama et al.[15–17] succeeded in measuring the concentration of lattice oxygen by the hot gas extraction method, and they concluded that the

* Corresponding author. Fax: +81-427-21-3624.
E-mail address: hiroshi-yokota@denka.co.jp (H. Yokota).

0955-2219/02/$ - see front matter
PII: S0955-2219(02)00074-2

point defects in the β-Si_3N_4 crystal lattice that are created by oxygen dissolution dictate the thermal conductivity.

There are thus different results and considerations for the relation between grain size and the thermal conductivity of β-Si_3N_4. Kitayama et al.[18] demonstrated both theoretically and experimentally that the grain growth alone cannot improve the thermal conductivity of β-Si_3N_4. Hirosaki et al.[10] reported that a portion of the aluminum and oxygen in the liquid phase of the Y_2O_3–Al_2O_3 additive system dissolved into β-Si_3N_4 grains to form a solid solution of β′-SiAlON. This lowered the thermal conductivity because the dissolved aluminum and oxygen acted as point defects to scatter phonons. The effect of the impurities in grains of sintered β-Si_3N_4, which form point defects and dislocations, and the grain growth on the thermal conductivity has not yet been clarified. It is, however, highly possible that the grain size of β-Si_3N_4 affects the thermal conductivity if β-Si_3N_4 grains are purified during sintering.

The purpose of this study is to investigate the effect of impurities in the β-Si_3N_4 grains on the thermal conductivity of sintered Si_3N_4 ceramics.

2. Experimental procedure

High-purity raw Si_3N_4, powder (Grade NP-400, Denki Kagaku Kogyo, Tokyo, Japan), was obtained by direct nitridation of silicon. Table 1 shows properties of raw β-Si_3N_4 powder. Powders of β-Si_3N_4 and 8 wt.% Y_2O_3 (purity > 99.9%, BET 4 $m^2\ g^{-1}$, Shin-etsu Chemical, Tokyo, Japan) and 1 wt.% HfO_2 (purity > 99.9%. BET 4 $m^2\ g^{-1}$. Soekawa Chemical, Tokyo, Japan) were ball-milled for 3 h using methanol as the liquid. In the present work. HfO_2 was added to obtain a dense sintered material. The powder mixtures were subsequently dried and prepared for sintering. Approximately 110 g of the dried powder was uniaxially pressed under 20 MPa in a die 12.5 mm in diameter. The pellet was then isostatically cold-pressed under a pressure of 200 MPa. The CIPped pellet was placed in a BN crucible. Sintering was performed in a graphite furnace at 1900 °C for 8 and 48 h, respectively, under a nitrogen pressure 0.9 MPa.

Table 1
Properties of raw Si_3N_4 powder

Property	Value
α-Phase content (wt.%)	48.5
Carbon impurity (wt.%)	0.11
Calcium impurity (ppm)	230
Iron impurity (ppm)	710
Aluminum impurity (ppm)	80
Oxygen impurity (wt.%)	0.87
Average particle size (μm)	0.35
BET specific surface area ($m^2\ g^{-1}$)	19.7

The densities of specimens were measured by the Archimedes method. The microstructure of the sintered materials was examined by scanning electron microscopy (SEM, JSM-820, Jeol, Japan) of polished and plasma-etched surfaces. The weight loss of the green bodies after the sintering was measured.

Approximately 100 g of each body sintered for 8 and 48 h was ground using agate mortar and pestle until the crushed body passed through a 120-mesh sieve. The screened powders were subsequently etched by dissolving the grain boundary phases. The screened powders were then subjected to four successive rinse treatments. (1) A mixed solution of concentrated HF and HNO_3 at 60 °C for 3 h to dissolve the residual glassy phase, (2) a concentrated H_2SO_4 solution at 180 °C for 3 h to eliminate yttrium and hafnium compounds, (3) a dilute HF solution for 30 min using an ultrasonic vibrator to dissolve the SiO_2 film formed on the particle surfaces, and (4) a concentrated NH_4OH solution at 60 °C for 3 h to remove the Hf adsorbed onto the surface. Each treatment was similar to that reported by Hirano et al.[19] but more severe in the treatment to remove the grain boundaries. (Six repetitions were performed in each treatment.) After these treatments, the screened powders were classified using a centrifugal sedimentation method. Large grains were classified as those greater than 1 μm in diameter and small grains as those less than 1 μm in diameter. The classified powders were dried at 120 °C for 24 h. Lattice oxygen of β-Si_3N_4 was measured by a method developed by Kitayama et al.[16] The lattice oxygen content (wt.%) of the loose grains was measured ($n = 5$) using a commercial oxygen analyzer (Model TC-436, Leco Corp., St. Joseph, MI). Approximately 20 mg of the loose grains was weighed into a graphite crucible, and 200 mg of graphite powder (Product 501-073, LECO Co.) was added to the specimens to accelerate the carbothermal reduction of the oxide phase. The crucible was heated to 2500 °C in 5 min in a flowing argon atmosphere. The release of oxygen and nitrogen, as a function of temperature, and the total concentrations of oxygen and nitrogen were recorded. A total of three measurements were performed for each specimen. Acid decomposition of approximately 200 mg of the large and small Si_3N_4 grains was carried out in a HF/HNO_3 mixture in beakers on a hot plate at 160 °C for 16 h, the solution was subsequqently analyzed ($n = 5$) for impurities using the inductively coupled plasma (ICP-AES) method (Model ICAP-575 Nippon Jarrell Ash, Tokyo, Japan). Since yttrium and hafnium used as additives were detected (< 0.5 ppm) in all the loose grains of the specimens, the grain boundaries were almost removed from β-Si_3N_4 grains. The phase of the sintered materials was identified performed using X-ray diffractometry (XRD) (Cu K_α radiation, operating

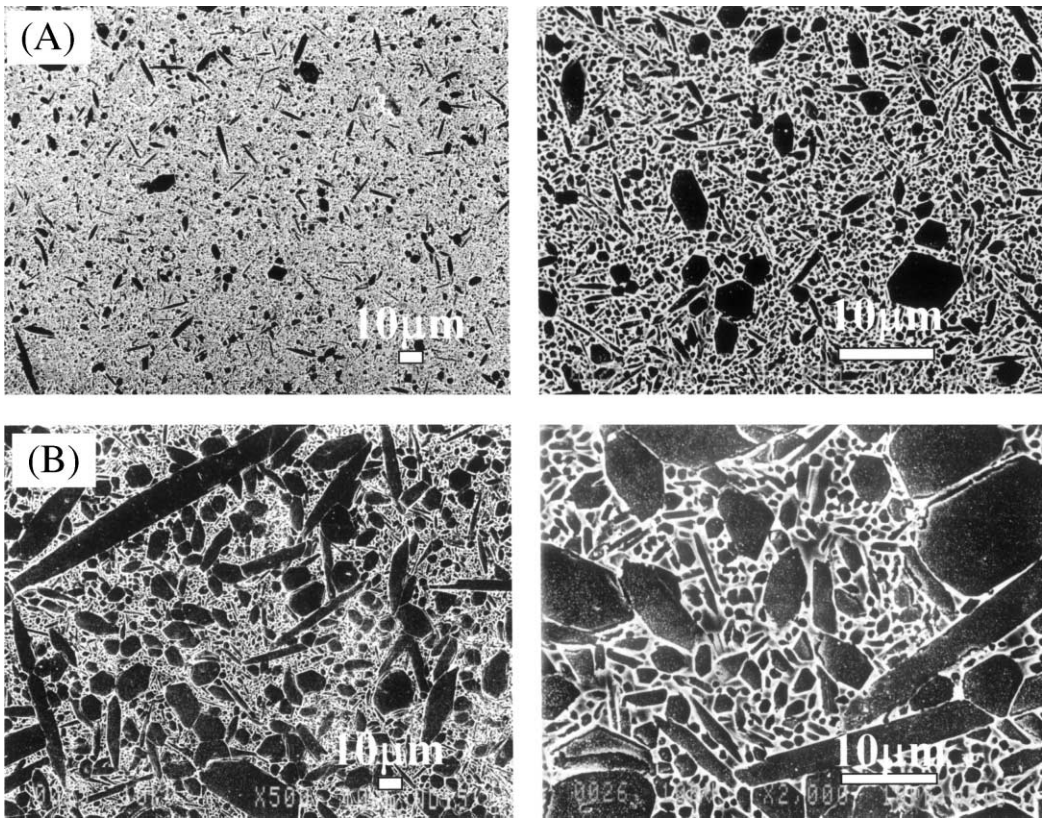

Fig. 1. SEM photographs of specimens sintered at 1900 °C (A) 8 h (B) 48 h.

conditions of 40 kV and 100 mA). To evaluate the thermal conductivity, disks 10 mm in diameter and 3 mm in thickness were cut from sintered materials. Thermal conductivity at room temperature was calculated from the following equation.

$$K = \alpha C_p \rho \quad (1)$$

The thermal diffusivity (α) and the specific heat (C_p) of the specimens were measured at room temperature by a laser-flash method using a thermal constant analyzer (TC-3000, ULVAC, Japan). A specific heat of 0.67 J/g·K was used in the present work).[10] The diameters of 1000 loose grains in each classified specimen were measured and recorded by scanning electron microscope (SEM).

3. Results and discussion

Fig. 1 shows the effect of the sintering time on the microstructure of Si_3N_4 after being sintered at 1900 °C for 8 and 48 h, respectively. The specimens had a bimodal microstructure composed of small matrix grains and large elongated grains. The matrix grains were 0.3–2 μm in diameter, and 1–6 μm in length, and the large grains were 2–15 μm in diameter and 10–160 μm in length. The area fraction of large grains ($\geqslant$2 μm in diameter) increased with increasing sintering time.

After sintering, the smaller matrix grains were separated from the larger grains by classification. Fig. 2 shows photographs of grains sintered for 48 h after classification. Matrix grains were less than 1 μm in diameter, and large grains were greater than 1 μm in diameter.

Table 2 summarizes the results of the density of sintered materials, weight loss and the XRD phase identification for the specimens sintered at 8 and 48 h. For the specimen sintered at 8 h, the $YSiO_2N$ (Y_2O_3:SiO_2:-Si_3N_4 = 2:1:1) and $Y2Hf_2O_7$ phases were observed, and the corresponding Y_2O_3:SiO_2 ratio was 2:1. For the specimen sintered at 48 h, the $Y_2Si_3N_4O_3$ (Y_2O_3:SiO_2:Si_3N_4 = 1:0:1) and $Y_2Hf_2O_7$ phases were observed, and the corresponding Y_2O_4:SiO_2 ratio was 1:0. In the Si_3N_4–Y_2O_3–SiO_2 ternary phase diagram, the $YSiO_2N$ phase is on the $Y_{20}Si_{12}N_4O_{48}$ (Y_2O_3:SiO_2:Si_3N_4 = 10:9:1)–$Y_2Si_3N_4O_3$ tie line. Therefore, it is considered that $YSiO_2N$ phase reveals the middle stage of the grain boundary phase to the $Y_2Si_3N_4O_3$ phase, for which the Y_2O_3/SiO_2 ratio is higher when sintering time increased. Table 2 also shows the weight loss of both specimens, the weight loss of the specimen sintered 48 h was approximately twice that of the specimen sintered for 8 h. It is considered that this large weight loss and the change in the composition of the grain boundary phase with the long sintering time are attributed to evaporation of SiO_2 [SiO (g)] from the oxynitride phase ($YSiO_2N$) by the following chemical reaction;

$$Si_3N_4\ (s) + 3SiO_2(1) \rightarrow 6SiO(g) + 2N_2\ (g) \quad (2)$$

Kitayama et al.[16] concluded that the grain boundary phase composition dictated the lattice oxygen content of β-Si_3N_4. The lattice oxygen content was lowest when both $Y_{20}Si_{12}N_4O_{48}$ and $Y_2Si_3N_4O_3$ were present in the grain boundary phase. It is, therefore, expected that the $YSiO_2N$ phase as well as the $Y_2Si_3N_4O_3$ phase should be present in the grain boundary phase of β-Si_3N_4 that has been sintered with Y_2O_3 to guarantee high thermal conductivity. Thus, this composition change of the grain boundary phase ($YSiO_2N \rightarrow Y_2Si_3N_4O_3$) is considered to remove the lattice oxygen.

Table 3 shows the result of impurities in the crystal lattice and also the thermal conductivity of the sintered specimens. The impurities of Si_3N_4 detected in the grains with concentrations $\geqslant 1$ ppm were oxygen, aluminum, iron and calcium. The thermal conductivity of Si_3N_4 at room temperature increased from 88 to 120 $Wm^{-1}\ K^{-1}$ as the impurities in the grains decreased. In αSi_3N_4 it is common for nearly all of the grains to undergo a transformation to β-Si_3N_4. It is also well known that even in β-Si_3N_4 the relatively small β-particles in the raw material powder undergo a dissolution and reprecipitation onto the large β-nuclei. In the present work, since the fine size and 48.5 wt.% content of α-Si_3N_4 powder was used, it is expected that many grains, not only in particular small α-particles but also small β-particles in the raw material powders, undergo dissolution and reprecipitation by the liquid phase. The fact that the coarse grains have less dissolved oxygen impurity than the fine grains, as shown in Table 3, strongly suggest that purification occurred in particular with the grain growth.

Table 3 also shows that lattice oxygen was the major impurity in the grains. Oxygen content remained

Table 2
Results of density, weight loss and grain boundary phase identification via XRD for specimens sintered at 8 and 48 h

Specimen (h)	Density (g cm^3)	Weight loss (wt.%)	Intensity of phases present			
			$Y_{20}S_{12}N_4O_{48}$ Y_2O_3:SiO_2 = 10:9	$YSiO_2N$ Y_2O_3:SiO_2 = 2:1	$Y_2Si_3N_4O_3$ Y_2O_3:SiO_2 = 1:0	$Y_2Hf_2O_7$
8	3.322	2.43	(X)	X X	(X)	XX
48	3.301	4.53	((X))	X	XX	XX

Table 3
Impurities in crystal lattice of Si_3N_4

	8 h		48 h	
	Large	Small	Large	Small
Impurities element				
Oxygen (ppm)	980±70	1900±160	460±30	1920±200
Aluminum (ppm)	98±5	101±5	95±4	98±4
Calcium (ppm)	50±3	53±3	2±1	10±1
Iron (ppm)	10±1	50±1	<1	<1
Average diameter (μm)	0.92±0.37	0.70±±0.28	12.10±0.75	0.87±0.32
Thermal conductivity ($Wm^{-1}\ K^{-1}$)	88±1		120±1	

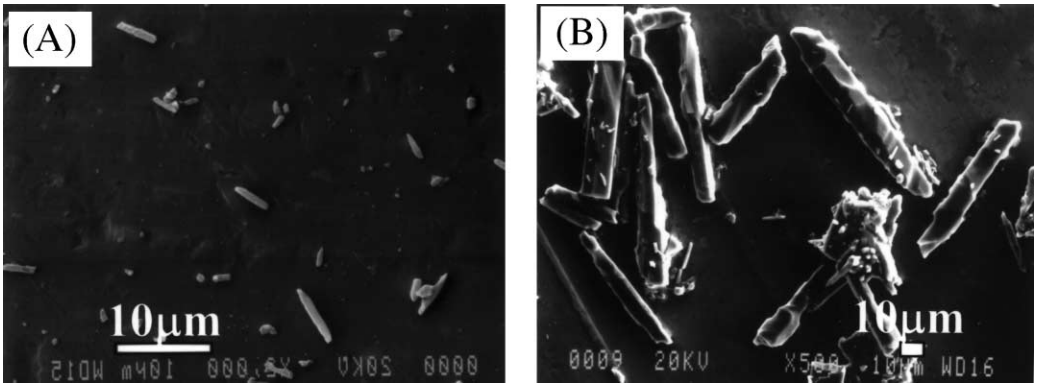

Fig. 2. SEM photographs of disintegrated specimens sintered at 1900 °C for 48 h (A) matrix grains (B) large grains.

constant at approximately 2000 ppm for the smaller Si_3N_4 grains, but decreased to 500 ppm with annealing time as the grains grew.

Since iron and calcium, the impurities in the raw powder, were easily removed from both small and large grains with annealing time, it is clear that the grain boundary phase plays a role in the purification process. Purification by dissolution and reprecipitation with the grain growth was particularly remarkable for diameter of $\leqslant 1$ μm and then gradually purified up to 10 μm in diameter, and the degree of purification depended on the kind of impurity.

It should be noted that no purification had occurred for aluminum, which was independent of grain growth. This suggests that even with grain boundary phases that are compatible with alumina, it was not removed from the Si_3N_4 lattice despite dissolution and reprecipitation. It is known that the dissolved aluminum and oxygen form a solid solution of β′-SiAlON. Two possible reasons can be considered for the inability to remove aluminium. One is due to the stability of the β′-SiAlON in β-Si_3N_4 lattice rather than forming the liquid phase of Y_2O_3–Al_2O_3. Another explanation may be the thermodynamic stability of yttrium-based phases with $YSiO_2N$ or the $Y_2Si_3N_4O_3$ phases being more stable than yttrium-aluminate phases, although aluminum can be incorporated into both $YSiO_2N$ and $Y_2Si_3N_4O_3$ phases.

As mentioned above, the thermal conductivity of the sintered material increased from 88 to 120 Wm^{-1} K^{-1} with annealing time. It may perhaps be argued that the increase in the thermal conductivity may be related to the grain growth. Watari et al.[14] reported the calculated phonon mean free path of sintered β-Si_3N_4 materials was approximately 20 nm at room temperature, which is very small as compared to the grain size. Hence, little effect of the grain size on thermal conductivity is expected. A simplistic picture is that the increase in the thermal conductivity of β-Si_3N_4 is attributed not to the grain size itself but to purification of β-Si_3N_4 grains occurring during grain growth by dissolution-reprecipitation. Smaller grains, originally impure (containing a higher concentration of oxygen), can dissolve in the liquid phase and deposit as a purified β-Si_3N_4 on large elongated grains. It should be realized that the composition and dihedral angle of the grain boundary phases will play a significant role in the thermal conductivity of the sintered ceramics. As a result, the thermal conductivity increased from 88 to 120 Wm^{-1} K^{-1}. Since aluminum is not removed from the β-Si_3N_4 lattice, the use of high-purity Si_3N_4 with a low amount of aluminum is recommended to further increase the thermal conductivity. However, impurity contents in hundreds of ppm result in the range of 10^{17}–10^{19} defects/cm^3 and yields substitutional solute ions, as well as the associated charge compensating defects, in virtually every unit cell, thereby limiting the phonon mean free path to unit cell dimensions. It is, therefore, likely that the nearly 50% increase in thermal conductivity due to not only a reduction of point defect concentration but also to something else contributing. For example, grain growth by dissolution and precipitation would presumably yield new grains with significantly lower line and planar defect concentrations. It is possible that a lower concentration of defects such as dislocations and twins is also playing a role in the refined and presumable recovered, microstructures. The composition of the grain boundary phase is also changing as a function of time. Grain boundary film thickness,[17] grain boundary phases,[18] and amount of secondary phases[17] all affect thermal conductivity. Thus the relation between the concentration of defects and thermal conductivity is an oversimplification of the overall picture.

4. Conclusions

The effect of impurities in the crystal lattice and microstructure on thermal conductivity of sintered Si_3N_4 was investigated using high-purity β-Si_3N_4 powder. The sintered materials were fabricated by gas pressure sintering a 1900 °C for 8 and 48 h with the addition of 8 wt.% Y_2O_3 and 1 wt.% HfO_2. Subsequently a chemical analysis was performed on the sintered loose grains after the grain boundaries were removed. From the present work, the following conclusions were drawn:

1. The impurities of Si_3N_4 detected in the crystal lattice were oxygen, aluminum, iron and calcium, whiceh originated from impurities in the raw β-Si_3N_4 powder.
2. Aluminum was not removed from Si_3N_4 grains despite the dissolution and reprecipitation process.
3. The coarse grains contained less oxygen, iron, and calcium impurities content than the fine grains. Iron and calcium impurities in the raw powder were easily removed from the grains during grain growth.
4. Oxygen was the major impurities in the grains, and decreased with grain growth. Oxygen content was a strong function of grain size, with larger grains having lower oxygen content.
5. The thermal conductivity of Si_3N_4 ceramics increased from 88 (8 h) to 120 Wm^{-1} K^{-1} (48 h) as the impurities in the crystal lattice of β-Si_3N_4 decreased.
6. Purification by grain growth thus improved the thermal conductivity, but the changing grain boundary phases might also influence the thermal conductivity.

References

1. Haggerty, J. S. and Lightfoot, A., Opportunities for enhancing the thermal conductivities of SiC and Si_3N_4 ceramics through improved processing. *Ceram. Eng. Sci. Proc.*, 1995, **16**(4), 475–487.

2. Watari, K., Li, B.-C., Pottier, L., Foumier, D. and Toriyama, M.Thermal conductivity of β-Si_3N_4 single crystal. *Key Eng. Mater. (Electroceramics in Japan III), 2000, 181–182.*
3. Ziegler, G. and Hasselman, D. P., Effect of phase composition and microstructure on the thermal diffusivity of silicon nitride. *J. Mater. Sci.*, 1981, **16**, 495–503.
4. Hirai, T., Hayashi, S. and Niihara, K., Thermal diffusivity, specific heat and thermal conductivity of chemically vapor-deposited Si_3N_4. *Am. Ceram. Soc. Bull.*, 1978, **57**(12), 1126–1130.
5. Kuriyama, M., Inomata, Y., Kujima, T. and Hasegawa, Y., Thermal conductivity of hot-pressed Si_3N_4 by the laser flash method. *Am. Ceram. Soc. Bull.*, 1978, **57**(12), 1119–1122.
6. Tsukuma, K., Shimada, M. and Koizumi, M., Thermal conductivity and microhardness of Si_3N_4 with and without additives. *Am. Ceram. Soc. Bull.*, 1981, **60**(9), 910–912.
7. Watari, K., Seki, Y. and Ishizaki, K., Thermal conductivity of HIP-sintered silicon nitride, properties of HIP sintered silicon nitride. *J. Ceram. Soc. Jpn.*, 1989, **97**(1), 56–62.
8. Watari, K., Seki, Y. and Ishizaki, K., Thermal properties of HIP sintered silicon nitride. *J. Ceram. Soc. Jpn.*, 1989, **97**(1), 74–81.
9. Hirosaki, N., Okamoto, Y., Ando, M., Munakata, F. and Akiume, Y., Thermal conductivity of gas-pressure-sintered silicon nitride. *J. Am. Ceram. Soc.*, 1996, **79**(11), 2878–2882.
10. Hirosaki, N., Okamoto, Y., Ando, M., Munakata, F. and Akiume, Y., Effect of grain growth on the thermal conductivity of silicon nitride. *J. Am. Ceram. Jpn.*, 1996, **104**(1), 49–53.
11. Hirao, K., Watari, K., Brito, M. E., Toriyama, M. and Kanzaki, S., High thermal conductivity in silicon nitride with anisotropic microstructure. *J. Am. Ceram. Soc.*, 1996, **79**(9), 2485–2488.
12. Watari, K., Hirao, K., Brito, M. E., Toriyama, M. and Kanzaki, S., Hot isostatic pressing to increase thermal conductivity of silicon nitride ceramics. *J. Mater. Res.*, 1999, **14**(4), 1538–1541.
13. Akiume, Y., Munakata, F., Matsuo, K., Okamoto, Y., Hirosaki, N. and Satoh, C., Effect of grain size and grains structure on the thermal conductivity of β-Si_3N_4. *J. Ceram. Soc. Jpn.*, 2000, **83**(8), 1985–1992.
14. Watari, K., Hirao, K., Brito, M. E., Toriyama, M. and Ishizaki, K., Effect of grain size on the thermal conductivity of silicon nitride. *J. Am. Ceram. Soc.*, 1999, **82**(3), 777–779.
15. Kitayama, M., Hirao, K., Tsuge, A., Toriyama, M. and Kanzaki, S., Oxygen content in β-Si_3N_4 crystal lattice. *J. Am. Ceram. Soc.*, 1999, **82**(11), 3263–3265.
16. Kitayama, M., Hirao, K., Tsuge, A., Watari, K., Toriyama, M. and Kanzaki, S., Thermal conductivity of β-Si_3N_4. Part II, effect of lattice oxygen. *J. Am. Ceram. Soc.*, 2000, **83**(8), 1985–1992.
17. Kitayama, M., Hirao, K., Toriyama, M. and Kanzaki, S., Thermal conductivity of β-Si_3N_4. Part I, effects of various microstructural factors. *J. Am. Ceram. Soc.*, 1999, **82**(11), 3105–3112.
18. Kitayama, M., Hirao, K., Watari, K., Toriyama, M. and Kanzaki, S., Thermal conductivity of β-Si_3N_4: III, effect of rare-earth (RE = La, Nd, Gd, Y, Yb, and Sc) oxide additives. *J. Am. Ceram. Soc.*, 2001, **84**(2), 353–358.
19. Hirao, K., Tsuge, A., Brito, M.E. and Kanzaki, S. Preparation of rod-like β-Si_3N_4 single crystal particles, 1994. In *Key Engineering Materials*, 89–91. Trans Tech Publications, Switzerland, pp. 63–66.